SEMARAK ILMU PUBLISHING

Journal of Advanced Research in Fluid Mechanics and Thermal Sciences

Journal homepage:
https://semarakilmu.com.my/journals/index.php/fluid_mechanics_thermal_sciences/index
ISSN: 2289-7879

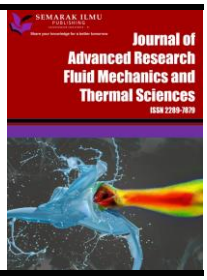

Simulating the Rising Air Bubbles Stream through Heavy Fuel Oil Residue Bubble Column Reactor using COMSOL

Hussein Reda Muhammad Ali Al-Naqqash[1], Mohammed Alhwayzee[2], Farhan Lafta Rashid[2,*]

[1] Mechanical Engineering Department, University of Kerbala, Karbala 56001, Iraq
[2] Petroleum Engineering Department, University of Kerbala, Karbala 56001, Iraq

ARTICLE INFO

Article history:
Received 13 April 2024
Received in revised form 10 August 2024
Accepted 21 August 2024
Available online 15 September 2024

Keywords:
Air column; two phase flow; COMSOL Multiphysics; bubble rising; heavy fuel oil residue

ABSTRACT

Several industrial operations rely on the rise of air bubbles through heavy fuel oil residue (HFOr), including oil recovery and wastewater treatment. In order to increase efficiency and decrease expenses, it is necessary to understand the peculiarities of this process. With the help of COMSOL Multiphysics, we numerically simulate the ascent of a single air bubble via HFOr in this article. The dimensions of the container used in the simulations were (100) mm in diameter and (200) mm in height, with an air bubble diameter of 4.5 mm. For an air bubble ascending through an HFOr column, the predicted numerical outcomes are contrasted with nine experimental versions. As the bubble rose higher, the region with the greatest number of vortices was located on its side. The remaining vortex is contained inside the bubble. In addition, since drag decreases the flow, a lighter fluid usually exhibits a region of strong vortex and low pressure. Because of the oscillation effect, the results reveal that the rising velocity initially rises and then gradually falls between 0.6 and 0.65 s. The air bubbles' wavy motion is caused by the high fluid density, which becomes worse as the air velocity gets higher. The values of the drag coefficient rise sharply with decreasing air extrusion speed. It turns out that the height of the fluid has an inverse relationship with the pressure.

1. Introduction

Because of its useful features, gas-liquid bubble columns are often used as two-phase reactors in biological, chemical, and industrial processes, Heavy fuel oil (HFO) byproducts must undergo these essential industrial, chemical, and biological procedures in order to be recycled or treated in a way that reduces their environmental impact [1,2]. It could be difficult for bubbles to travel around in a column because to the high density to viscosity ratio [3]. Predicting the rate of bubble bursting using a variety of physical qualities and system parameters is another difficult mathematical problem [4]. Using state-of-the-art computational fluid dynamics, a processing capacity and technology, we have successfully analyzed rising air bubbles in vertical HFO columns [5].

* *Corresponding author.*
E-mail address: farhan.lefta@uokerbala.edu.iq

https://doi.org/10.37934/arfmts.121.1.7084

Both the surface force equation that is constant and the equation that governs the interface are [6]. In every step of their inter-tracking motion, both use VOF technology. The leveling strategy is used in conjunction with the liquid volume technique to improve bubble formation and interfacial pursuit [7]. Although studies have shown how air bubbles rise, the most challenging aspect is quantitative measurement due to the numerous problems revealed by multiphase-flow experiments [8,9]. When it comes to assessing ascending air bubbles in vertical HFO columns, computational fluid dynamics is one of the cutting-edge numerical methods and processing capacity that has proven effective [10]. The two-phase flow model was successfully executed using the VOF method [11]. The surface force equation that is continuous and the equation that governs the interface [12]. Both make use of the VOF method, which was used throughout the whole interfacial tracking motion process [13].

To enhance bubble form and interfacial pursuit, the fluid volume approach is used with the level-set (LS) methodology [14]. The relaxation equation and a common Hamilton-Jacobi equation are combined in a novel reinitialization approach that was suggested [15]. There is less quantitatively created interface distortion using the suggested approach as compared to earlier methods [16]. In addition, adding three dimensions to this method is not hard at all [17]. This technique also permits the spontaneous merging of contact lines at the spreading fluid interface [18].

Gas flow rate and mass concentration both effectuate a rise in detached and instantaneous volumes, whereas orifice diameter has the opposite effect [19-21]. The research discovered that the velocity in the vertical wake of an ascending isolated bubble differs significantly from the Gaussian distribution for isothermal and thermally stratified liquid layers [22,23]. Nozzle diameter is directly proportional to bubble size, according to the collected data [24]. The shape of the bubble changes as a result of different drag forces as the diameter increases [25]. From a Reynolds number of 10 to 0.05, the drag coefficient increases from 15 to 400.

Numerical evaluations of air bubble streams with diameters 3 mm rising in HFOr containers with diameter (100 mm) and height (200 mm) utilizing the seldom used COMSOL-Multiphysics are implemented in this study [26]. The results of this research could provide light on the real physical phenomena and the design of reactors for bubble columns. When it comes to the CFD simulation's multiphase flow model, it lastly offers additional selection criteria.

2. Methodology

2.1 Materials

The first part of this study is air, and the second part is HFOr. You may find a list of the fundamental physical parameters used to monitor and characterize air and HFOr in Table 1. This collection provides a solid foundation for comprehending the intricate dynamics and interactions of the HFOr and air components in the context of multiphase flow.

Table 1
Physico-chemical characteristics of the fluids evaluated under normal conditions

Fluid	Air	HFOr	Units
Density	1.22	965.7	Kg/m^3
Dynamic viscosity	$1.825x^{-5}$	0.17623	Pa.s
Surface tension	--	1.52040677	mN/m

2.2 Governing Equation

To determine the motion of air bubble through HFOr, it can be from [26-29]

$$\frac{\partial \phi}{\partial t} + u \cdot \nabla \phi = \gamma \nabla \left(\varepsilon \nabla \phi (1 - \phi) \frac{\nabla \phi}{|\nabla \phi|} \right) \quad (1)$$

In this equation, u represents the fluid velocity in m/s, γ is the reinitialization parameter in m/s, and ε=hc/2 which defines the interface thickness in m. The mesh of element with biggest size at the zone gone by the interface is indicated by the logo (hc), ϕ is the stage established, and its quantity ranged from 0 to 1. The fluid density and dynamic viscosity are also predicted using the level set function [30,31].

$$\rho = \rho_F + (\rho_A - \rho_F)\phi \quad (2)$$

$$\mu = \mu_F + (\mu_A - \mu_F)\phi \quad (3)$$

The constant viscosity and density of air and fuel are denoted by μ_A, μ_F, ρ_A, and ρ_F , respectively.

Ub is the fluid terminal velocity, which may be expressed as follows [32-35]

$$Ub = \sqrt{\frac{4(\rho_F - \rho_A) g Db}{3 C_D \rho_F}} \quad (4)$$

The drag coefficient is denoted by C_D, density by ρ, bubble diameter by Db, gravitational constant by g, and air or fuel represented by A and F [36-40].

$$Re = \frac{\rho_F U_b Db}{\mu_F} \quad (5)$$

where Re represents bubble's Re number.

2.3 Engineering Requirements and Parameters

One air bubble rising in a container of heavy fuel oil residue is studied in this study using a 2D field. According to Table 2 and Figure 1, the container has a width of 100 mm and a height of 200 mm. To begin the simulation, a nozzle with a diameter of 3 mm is introduced into the middle of the container and air is extruded at a speed ranging from 0.05 to 0.15 m/s. This causes air bubbles with a diameter of 4.5 mm to be created. As a result of atmospheric pressure and buoyancy, these air bubbles will rise inside the leftover heavy fuel oil.

Table 2
Geometrical specifications and parameters

Symbol	Value	Description
Dc	100 mm	Container diameter
H	200 mm	Container height
D_b	4.5mm	Bubble diameter
T	15.6°C	Temperature of system
γ	5 m/s	Reinitialization parameter

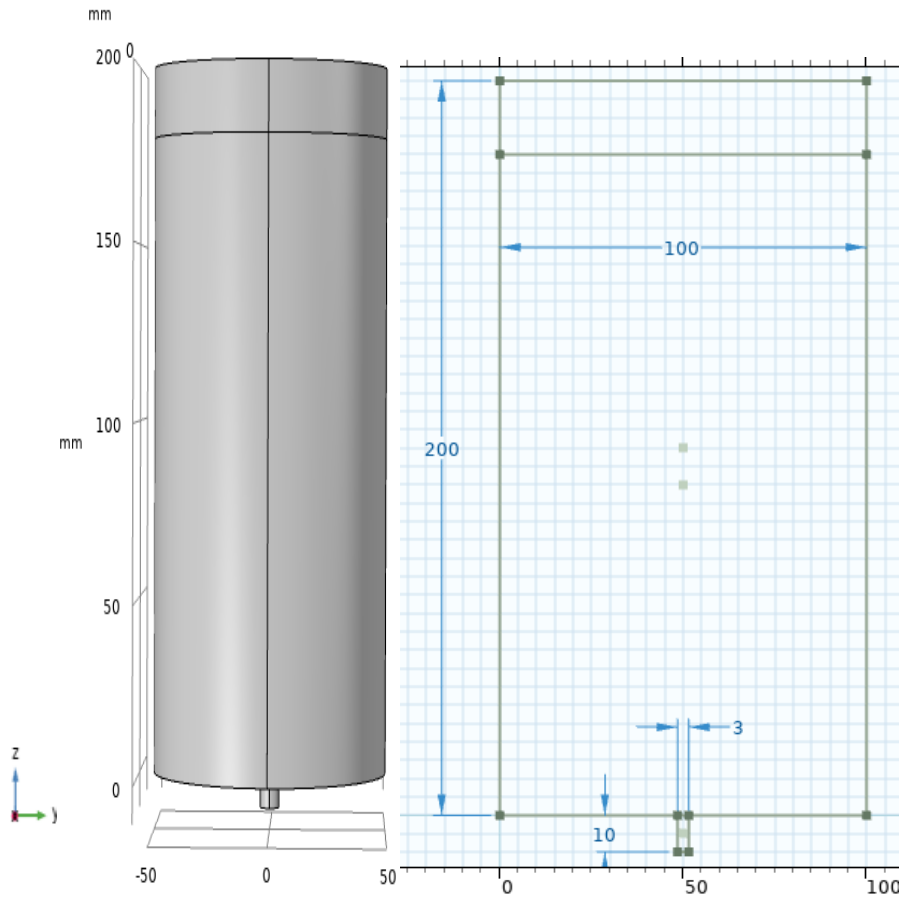

Fig. 1. Schematic diagram of the domain with geometric dimensions for a rising bubble of 4.5 mm diameter

2.4 Boundary Conditions and Numerical Techniques

The computational domain is bounded by no-slip boundaries at the sides and bottom, and by a pressure outlet boundary condition at the top. The reference operating pressure (101325 Pa), which is equivalent to the atmospheric pressure, is needed, and a gravitational acceleration (g) of 9.81 m/s^2 is given in the Y-direction. The simulations are conducted using the COMSOL-Multiphysics numerical framework, which resolves the volume fraction, continuity, and momentum equations. We employ the flow equations discretized at the second order upwind. The velocity-pressure coupling is resolved using the pressure implicit with the splitting operators (PISO) approach, which is selected for its fast convergence rate without compromising solution accuracy and stability. A body force-weighted approach is used to solve the pressure issue, and an implicit treatment of body forces is used to bolster the convergence of solutions. Based on an explicit approach with a time increment of 0.0001 s, the time-independent model is given a Courant number of 0.25.

This paper describes research that, in order to analyze bubble dynamics in multiphase flows, relies on a number of basic assumptions. These presumptions include

i. Understanding the Newtonian dynamics of water in a liquid state;
ii. Conditions in a steady state;
iii. Constant pressure gradient within the liquid;
iv. Isothermal operation;
v. The negligible interfacial tension between gas and liquid phases;
vi. Ideal gas behavior for air bubbles;

vii. Homogeneous fluid properties;
viii. Axisymmetric motion;
ix. Incompressible flow characteristics

2.5 Grid Dependency Test

To examine the effect of mesh size on outcomes, three different kinds of mesh were used. The dimensions of the cells in these meshes range from 0.25 mm by 0.25 mm to 0.35 mm by 0.35 mm. A structured mesh is shown in Figure 2. The graphic shows that normal, fine, and finer are the three distinct mesh resolutions. While a finer mesh will result in a more realistic simulation, it will also increase the computing time. It is the simulation's unique requirements that will dictate the mesh resolution.

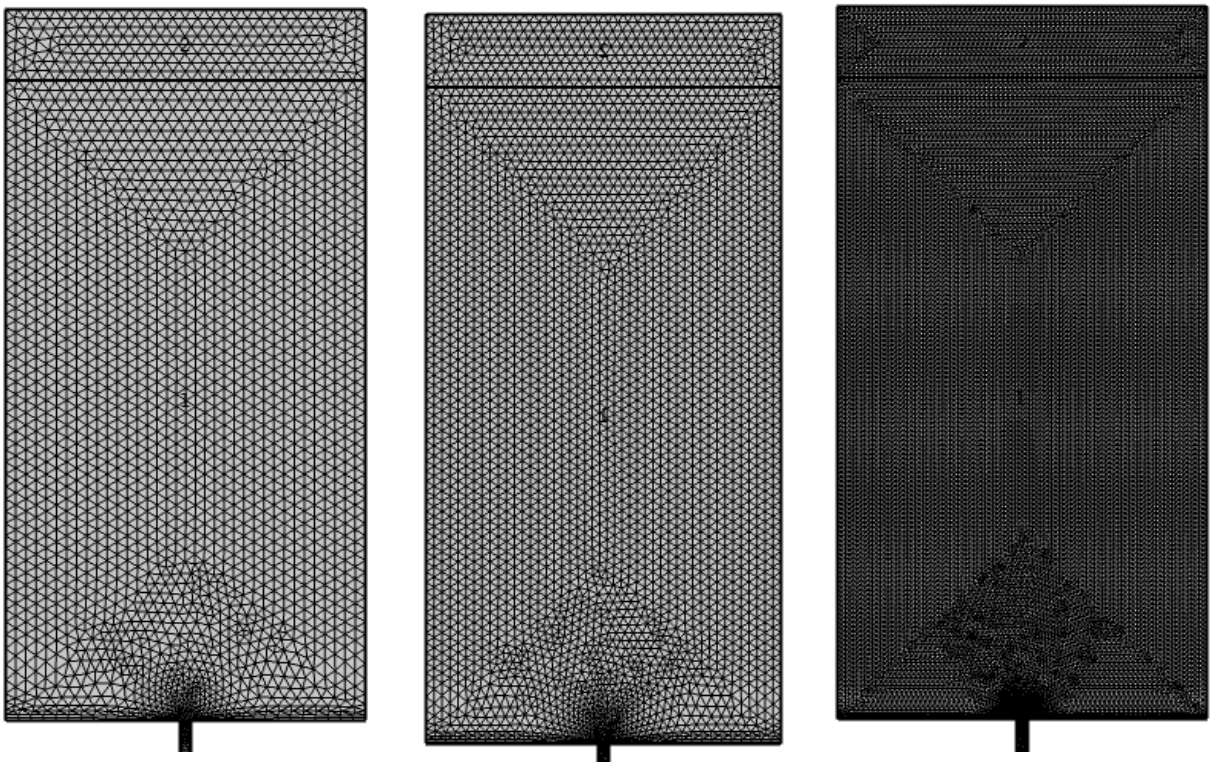

(a) normal (b) fine (c) finer

Fig. 2. Mesh generation

3. Results and Discussion

3.1 Validation

Confirming the found numerical insights required a thorough comparison with current models to guarantee the findings' validity and reliability. This study included comparing the predicted drag coefficients of several models with the Reynolds number (Table 3 is an exhaustive compilation of these models). The comparison between the model predictions and the numerical findings produced from the COMSOL simulations (current work) is shown in Figure 3 of this comprehensive evaluation. The primary objective was to ascertain the validity of the results by means of thorough cross-examination. The intrinsic necessity to ensure the consistency and numerical accuracy of the simulations, which supports the dependability of the findings, justifies this validation technique.

Table 3
Empirical correlations of Bubble drag coefficient

Turton and Levenspiel [41]	$C_D = \frac{24}{Re}(1 + 0.173Re^{0.657}) + \frac{0.413}{1+16300Re^{-1.09}}$
Mei and Klausner [42]	$C_D = \frac{16}{Re}\left(1 + \left(\frac{8}{Re} + \frac{1}{2}\left(1 + 3.315Re^{-\frac{1}{2}}\right)\right)^{-1}\right)$

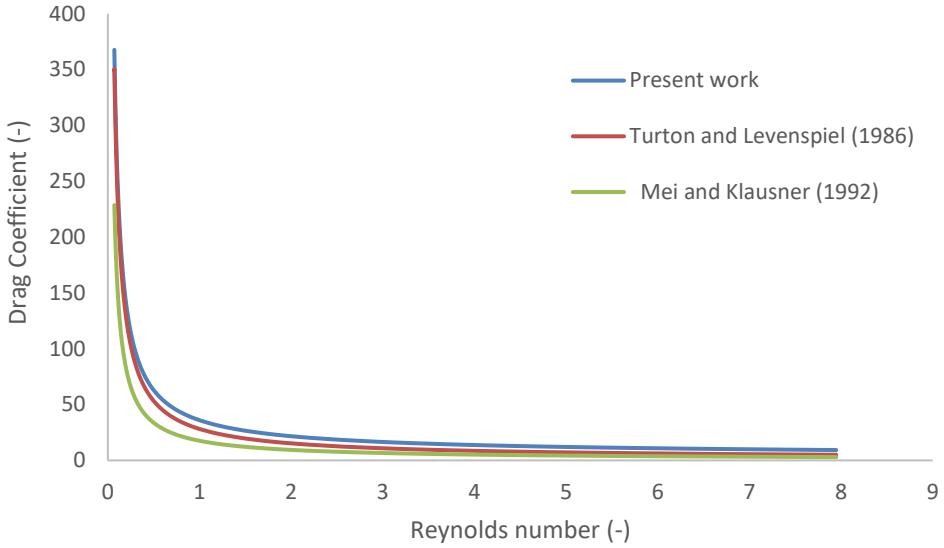

Fig. 3. Drag coefficient comparison from existing models vs. Reynolds number for validation with bubble diameter of 4.5 mm, height of 200 mm, and container diameter of 100 mm

A distinctive zigzag path guided by the laws of fluid dynamics results from the exact shaping of the bubble's surface by external field stresses, which produce an asymmetry in the pressure field along the bubble's border. In a fluid, ever-changing environment, this is the intricate dance of bubble behavior. The intriguing motion is shown in Figure 4, which shows the oscillatory or axis-reversing motions of the bubble as it travels along its zigzag path and ultimately reaches the domain's peak. A powerful liquid jet vortex occurs shortly after the bubble passes, which speeds up the upward motion and enhances form oscillations. This ascent provides an interesting dynamic.

As the air pour out of the nozzle, it inclines to adhere to the nozzle curve rather than separating from it right now. This generates a zone of low pressure in rear the nozzle, which doodles some of the air back towards the nozzle, establishing the recirculation zone. This recirculation region is caused by the Coanda effect.

The velocity of an air bubble increases with time, as shown in Figure 5. The oscillation effect causes the increasing velocity to peak for about 0.6 to 0.65 s before gradually decreasing. Lastly, the falling bubble velocity was found to be constant as the form oscillation reduced, after having risen in the spherical cap zone. From fluid transport dynamics to buoyancy-driven aeration system and process design, understanding the complex interactions of bubble motion, form oscillation, and equilibrium is critical. The results obtained from this detailed description have substantial practical and theoretical implications in many areas.

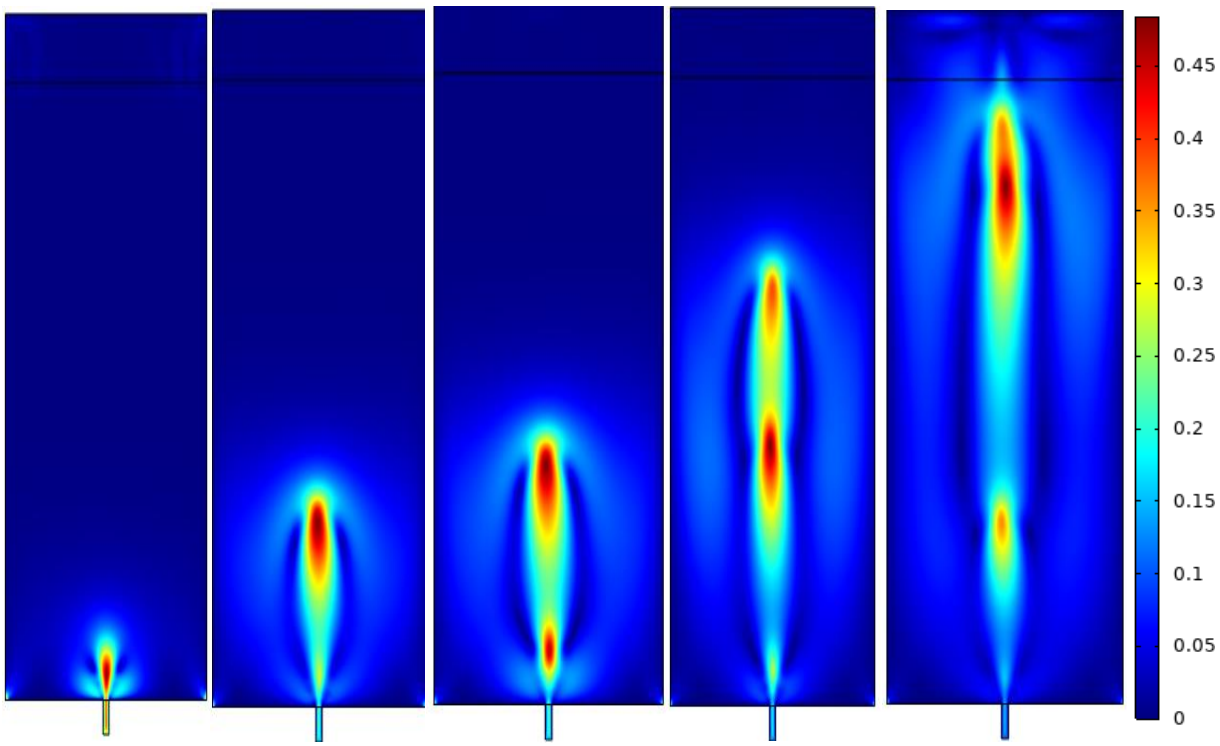

Fig. 4. Velocity contour with stream air from nozzle diameter of 3 mm, height and diameter of a container is 200 mm and 100 mm, respectively. (Time history from left to right are 0.32 s, 0.63 s, 0.71 s, 0.96 s, and 1.19 s, respectively, and U=0.1 m/s)

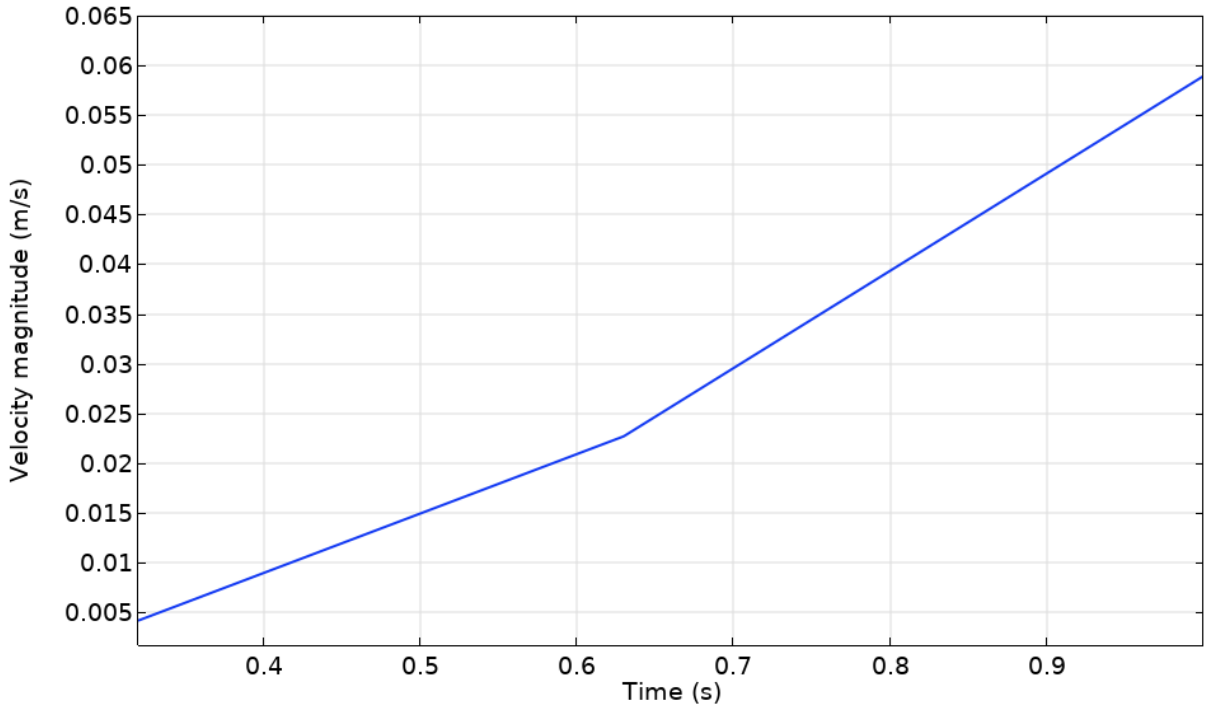

Fig. 5. Time-dependent velocity of a stream air rising in HFOr from nozzle diameter of 3mm, height and diameter of a container are 200 mm and 100 mm, respectively

Figure 6 shows that the container has a 200 mm diameter and a 100 mm height, appropriate for bubbles with a diameter of 4.5 mm. As they ascend, the air bubbles experience a gradual reduction in pressure. Because of this, the volume increases. This causes the bubbles to swell as they ascend in the air. Because it is buoyant and not subject to gravity, the hydrostatic pressure on the bubble drops

off as it rises in the liquid. This decrease in pressure leads the gas inside the bubble to expand, in accordance with Boyle's law, which states that, at a fixed temperature, the volume of a gas rises as the pressure it faces decreases. As an intriguing consequence of the cause-and-effect relationship between pressure and volume change, the size of the ascending bubbles increases as they climb. A gas bubble's volume attempts to equal the pressure outside it, which is consistent with its expansion. The pressure differential begins at about 4.19 Pascals and ends at around 0.15 Pascals when air is extruded from a 3 mm nozzle at a speed of 0.1 m/s over the duration of the (0.32-1.19) s time period. This points to a significant decline in pressure as time progresses. Figure 7 shows that the pressure is inversely related to the height of the fluid.

The volume proportion of air bubbles begins at around 0.21 and terminates at about 0.11, as shown in Figure 8. It seems that the volume fraction has been steadily decreasing. It seems like an exponential deterioration is shown in the plot. If the air bubbles are quickly escaping the solution, it might be because they are rising to the surface or becoming dissolved in the liquid around them.

Figure 9 displays the HFOr volume fraction, which exhibits a decreasing trend over time. Between 0.89 and 0.81 is where you may find the volume fraction of HFO. During the 8 seconds seen in the graph, there was a little shift. A consistent rate of change is suggested by the linear appearance of the figure.

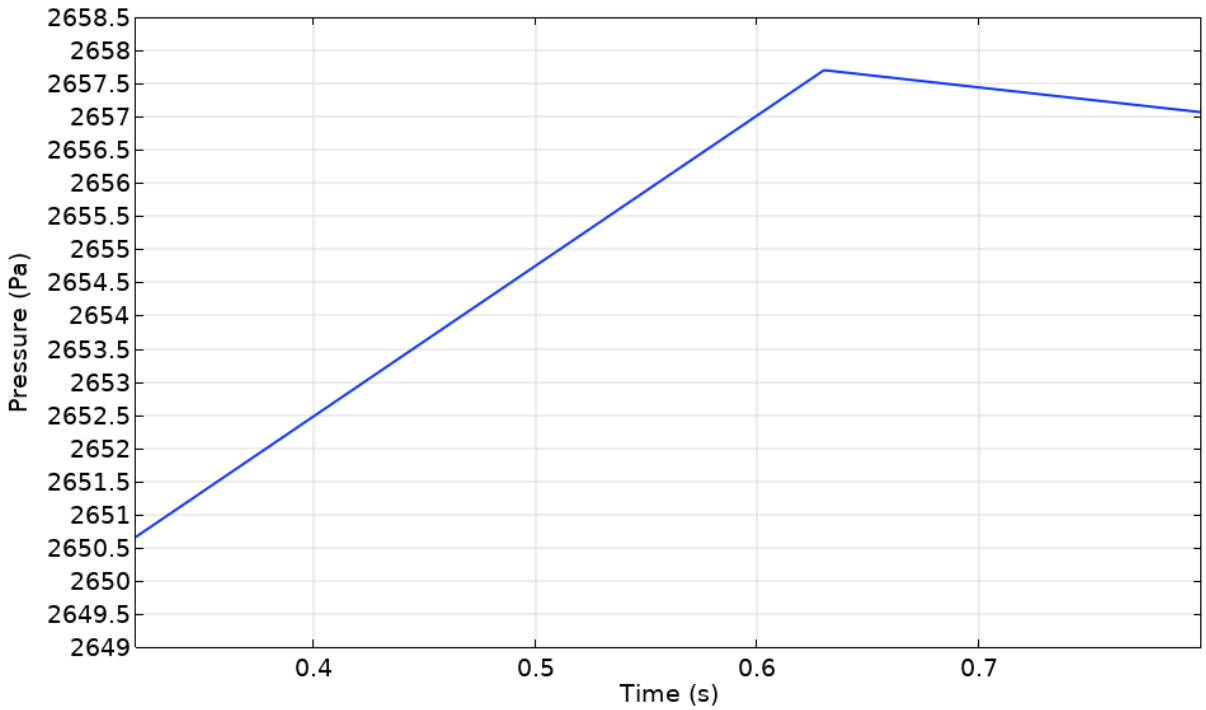

Fig. 6. Pressure of rising bubbles of 4.5 mm with time, height, and diameter of the container are 200 mm and 100 mm, respectively

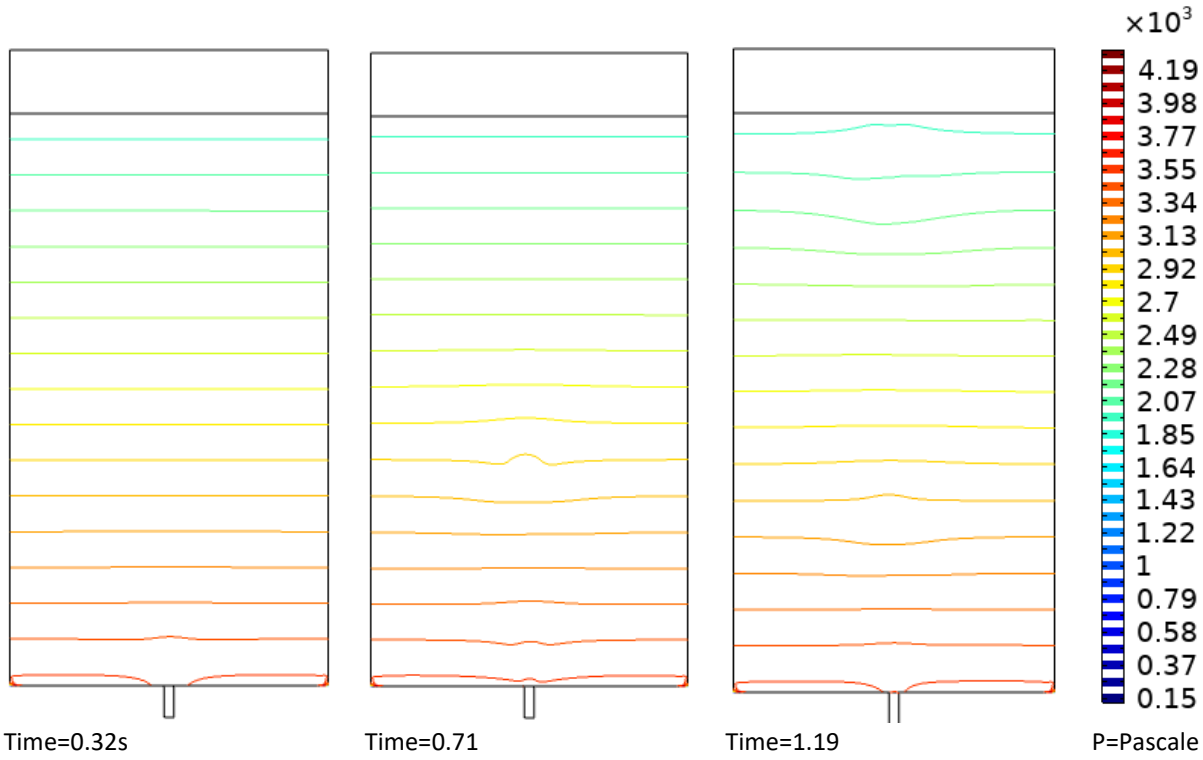

Fig. 7. The difference in pressure over a period of time (0.32-1.19)s

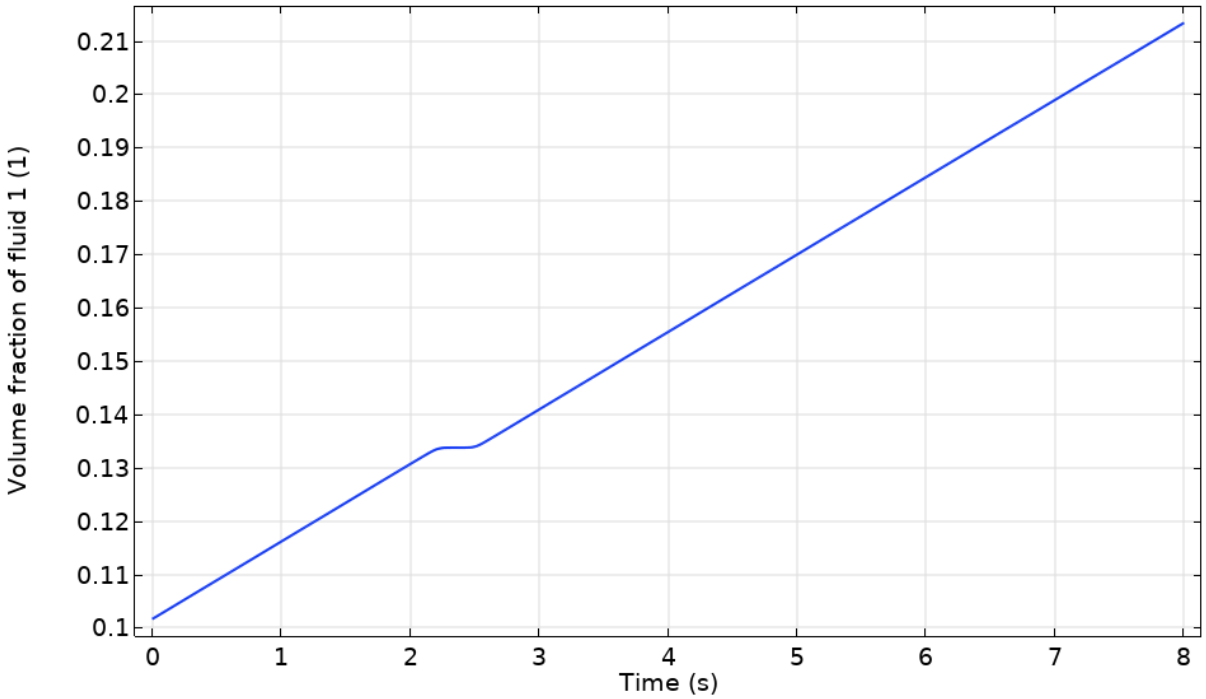

Fig. 8. Variation of volume fraction of air bubbles with time

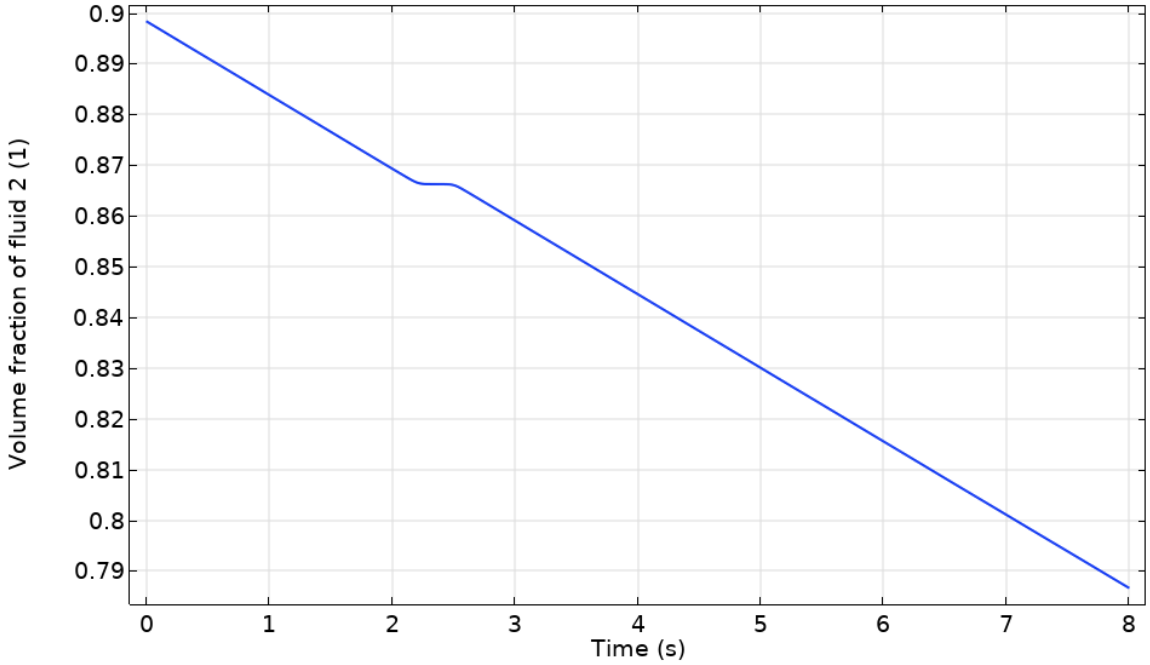

Fig. 9. Variation of volume fraction of HFOr with time

3.2 Variation of Pressure

As can be seen from the graph in Figure 10, the pressure grows in direct proportion to the height of the fluid column. This lines up with the idea that the pressure of a static fluid rises as one descends into the fluid. The reason for this is because the weight of the fluid above any given position causes pressure at that spot. The pressure increases in direct proportion to the height of the fluid column because the weight of the fluid above the place in question grows as the column rises. It would seem that the data points are linearly related, suggesting that the rate of change of pressure with respect to height is constant. This data points to a continuous fluid density over the whole height scale.

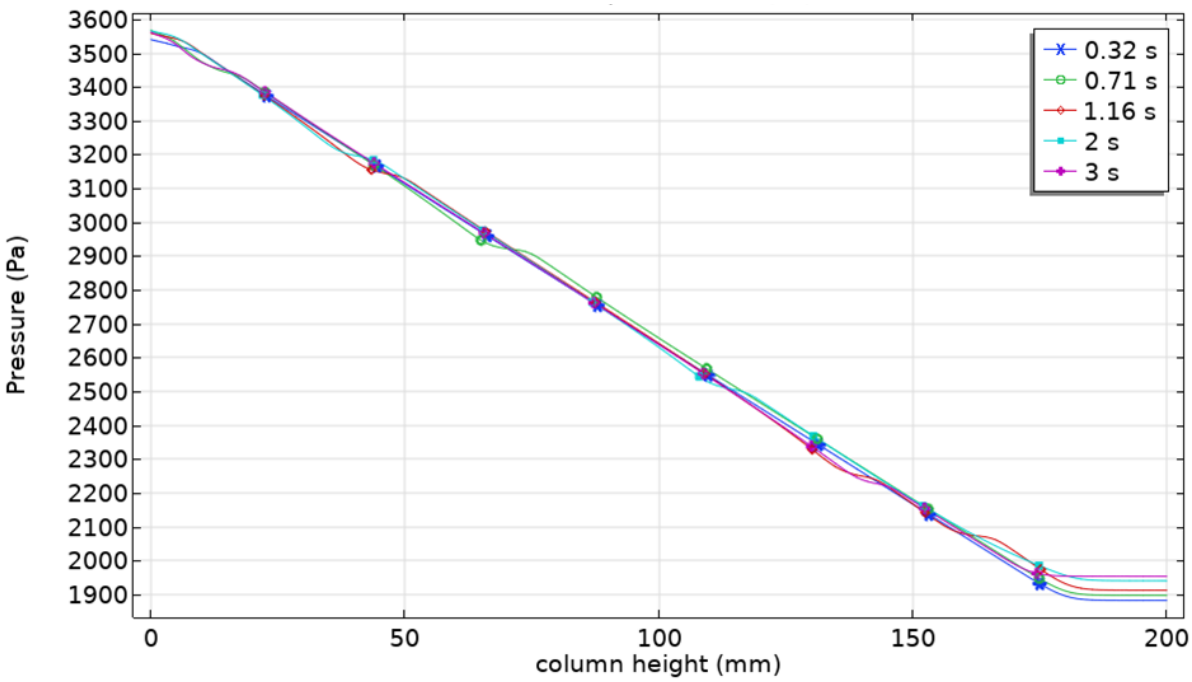

Fig. 10. Variation of pressure with fluid column height

3.3 Variation of Velocity with Reynolds Number

One dimensionless measure of the relative importance of inertial and viscous forces in a fluid's flow is the Reynolds number (Re). Flow regimes are classified and flow behavior is predicted using it. The Reynolds number is probably what defines the flow around the air bubble streams as they ascend through the liquid in Figure 11.

It is shown that the air bubble stream's velocity grows in relation to the Reynolds number. This indicates that the air bubble undergoes more acceleration and attains a faster velocity when inertial forces outweigh viscous forces. It seems like there is no linear link between Reynolds number and velocity. At small Reynolds numbers, the rate of acceleration with respect to Re is quite sluggish. The rate of velocity increase, however, is exponential at larger Reynolds numbers. Looking at the various flow regimes around the air bubble helps to understand this pattern: Viscous forces are the most important when the Reynolds number is small, usually less than 1. The drag coefficient, which measures the resistance to motion, is high around the bubble, and the flow around it is laminar. A gradual ascent is the outcome of this. Inertial forces are more significant when Reynolds numbers are larger, usually more than 1. If the bubble causes turbulence in the surrounding flow, the drag coefficient might drop. A more noticeable acceleration may result from this. A variety of variables, such as the bubble's dimensions and form, the liquid's characteristics (such as density and viscosity), and the existence of any outside forces (such buoyancy), determine the precise nature of the connection between the rising air bubble's velocity and Reynolds number.

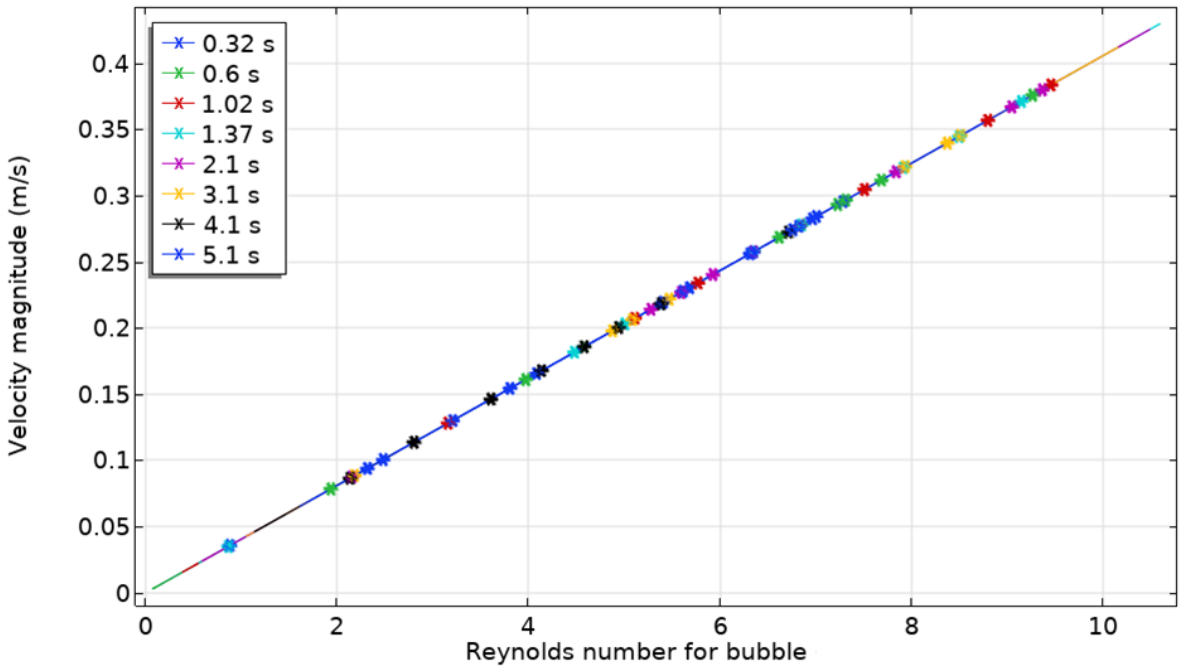

Fig. 11. Variation of velocity with Reynolds number of air bubble

3.4 Variation of Reynolds Number with Drag Coefficient

Figure 12 shows that the drag coefficient increased at values (15–400) as the Reynolds number value decreased (10–0.05) in the simulation. This figure shows the connection between the drag coefficient and the Reynolds number during the time (0.32-3) s for a 100 mm × 200 mm container. For tiny bubbles (less than around Re = 300), it is shown that the drag coefficient often drops as the Reynolds number increases. This indicates that the drag force experienced by tiny bubbles reduces

when inertial forces become more prevalent than viscous forces. The reason for this is because a small layer of liquid forms surrounding the bubble, reducing the total drag.

As bubble sizes increase beyond around Re = 300, the drag coefficient seems to stabilize at 2.6. It follows that the drag force acting on these bubbles eventually becomes Reynolds number independent. The reason for this is probably the presence of a continual drag force caused by the turbulent flow around the bubble and the breakdown of the thin liquid boundary layer.

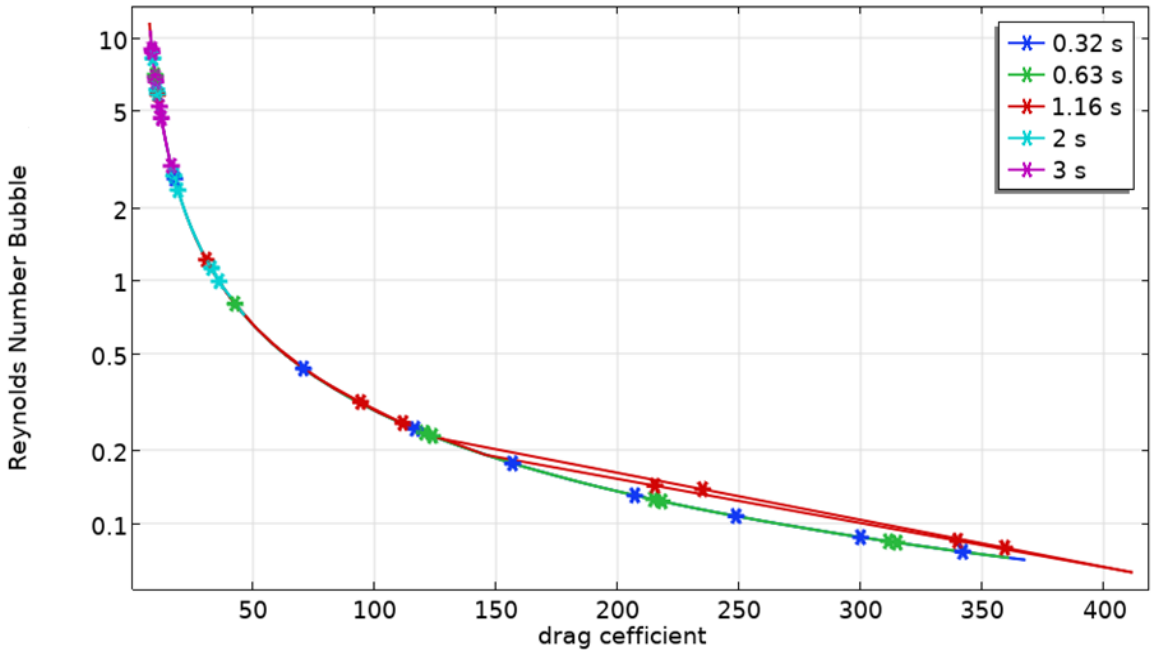

Fig. 12. Relationship of the Reynolds number with the drag coefficient for the period (0.32-3) s for a container with a diameter of 100 mm and a height of 200 mm

4. Conclusion

We used COMSOL-Multiphysics to investigate the gas-liquid two-phase flow numerically as air bubbles flowed through a stationary HFOr container. Results from a simulation of a stream of air bubbles passing through an HFOr column were compared to two empirical formulations. It seemed like everyone was on the same page. The study yielded the following important findings

i. As it makes its way up the domain, the bubble undergoes oscillatory or axis-reversing motions.
ii. The oscillation effect causes the growing velocity to peak for around 0.6 to 0.65 s before gradually decreasing. Lastly, the falling bubble velocity was found to be constant as the form oscillation reduced, after having risen in the spherical cap zone.
iii. When the air extrusion speed is increased, the bubbles split before they reach the surface.
iv. The air bubbles' wavy motion is caused by the high fluid density, which becomes worse as the air velocity gets higher.
v. The values of the drag coefficient rise sharply with decreasing air extrusion speed.
vi. As an intriguing consequence of the cause-and-effect relationship between pressure and volume change, the size of the ascending bubbles increases as they climb. A gas bubble's volume attempts to equal the pressure outside it, which is consistent with its expansion.

Acknowledgement
This research was not funded by any grant.

References

[1] Liu, Ming-yan, and Zong-ding Hu. "Studies on the hydrodynamics of chaotic bubbling in a gas-liquid bubble column with a single nozzle." *Chemical Engineering & Technology: Industrial Chemistry-Plant Equipment-Process Engineering-Biotechnology* 27, no. 5 (2004): 537-547. https://doi.org/10.1002/ceat.200401935

[2] Kulkarni, Amol A., and Jyeshtharaj B. Joshi. "Bubble formation and bubble rise velocity in gas− liquid systems: a review." *Industrial & Engineering Chemistry Research* 44, no. 16 (2005): 5873-5931. https://doi.org/10.1021/ie049131p

[3] Hassan, N. M. S., M. M. K. Khan, M. G. Rasul, and D. W. Rackemann. "Bubble rise velocity and trajectory in xanthan gum crystal suspension." *Applied Rheology* 20, no. 6 (2010): 65102.

[4] Hassan, N. M. S., M. M. K. Khan, and M. G. Rasul. "A modelling and experimental study of the bubble trajectory in a non-Newtonian crystal suspension." *Fluid Dynamics Research* 42, no. 6 (2010): 065502. https://doi.org/10.1088/0169-5983/42/6/065502

[5] Husseın, Emad Qasem, Farhan Lafta Rashıd, Ahmed Kadhım Husseın, and Obai Younıs. "Hydrodynamics of single bubble rising through water column using volume of fluid (VOF) method." *Journal of Thermal Engineering* 7, no. Supp 14 (2021): 2107-2114. https://doi.org/10.18186/thermal.1051642

[6] Dong, Zhiqiang, Weizhong Li, and Yongchen Song. "A numerical investigation of bubble growth on and departure from a superheated wall by lattice Boltzmann method." *International Journal of Heat and Mass Transfer* 53, no. 21-22 (2010): 4908-4916. https://doi.org/10.1016/j.ijheatmasstransfer.2010.06.001

[7] Zhang, Z. Y., L. A. Jin, S. Y. He, and Z. J. Yuan. "Study on coupling models for bubble floatation accompanied with heat and mass transfer." *Journal of Chemical Engineering of Chinese Universities* 32, no. 2 (2018): 358-367.

[8] Yoo, D-H., H. Tsuge, K. Terasaka, and K. Mizutani. "Behavior of bubble formation in suspended solution for an elevated pressure system." *Chemical Engineering Science* 52, no. 21-22 (1997): 3701-3707. https://doi.org/10.1016/S0009-2509(97)00216-9

[9] Xun, Ding Yudong Liao Qiang Zhu, and Wang Hong Liu Zhonghai. "Characteristics of Bubble Growth and Water Invasion at the Permeable Sidewall in Rectangular Liquid Flow Channel." *Journal of Mechanical Engineering* 49, no. 14 (2013): 119-124. https://doi.org/10.3901/JME.2013.14.119

[10] Du, Y. H., K. W. Xiong, Ying Zhang, X. T. Nie, M. Zhou, and C. B. Li. "Analysis of numerical simulation on horizontal arrangement equal bubbles rising." *Chinese Journal of Computational Mechanics 33* (2016): 889-894.

[11] Hirt, Cyril W., and Billy D. Nichols. "Volume of fluid (VOF) method for the dynamics of free boundaries." *Journal of Computational Physics* 39, no. 1 (1981): 201-225. https://doi.org/10.1016/0021-9991(81)90145-5

[12] Rabha, Swapna S., and Vivek V. Buwa. "Volume-of-fluid (VOF) simulations of rise of single/multiple bubbles in sheared liquids." *Chemical Engineering Science* 65, no. 1 (2010): 527-537. https://doi.org/10.1016/j.ces.2009.06.061

[13] Chakraborty, I., G. Biswas, and P. S. Ghoshdastidar. "A coupled level-set and volume-of-fluid method for the buoyant rise of gas bubbles in liquids." *International Journal of Heat and Mass Transfer* 58, no. 1-2 (2013): 240-259. https://doi.org/10.1016/j.ijheatmasstransfer.2012.11.027

[14] Szewc, Kamil, J. Pozorski, and J-P. Minier. "Simulations of single bubbles rising through viscous liquids using smoothed particle hydrodynamics." *International Journal of Multiphase Flow* 50 (2013): 98-105. https://doi.org/10.1016/j.ijmultiphaseflow.2012.11.004

[15] Ma, Dou, Mingyan Liu, Yonggui Zu, and Can Tang. "Two-dimensional volume of fluid simulation studies on single bubble formation and dynamics in bubble columns." *Chemical Engineering Science* 72 (2012): 61-77. https://doi.org/10.1016/j.ces.2012.01.013

[16] Buetehorn, Steffen, Dirk Volmering, Klaus Vossenkaul, Thomas Wintgens, Matthias Wessling, and Thomas Melin. "CFD simulation of single-and multi-phase flows through submerged membrane units with irregular fiber arrangement." *Journal of Membrane Science* 384, no. 1-2 (2011): 184-197. https://doi.org/10.1016/j.memsci.2011.09.022

[17] Yang, Ning, Zongying Wu, Jianhua Chen, Yuhua Wang, and Jinghai Li. "Multi-scale analysis of gas-liquid interaction and CFD simulation of gas-liquid flow in bubble columns." *Chemical Engineering Science* 66, no. 14 (2011): 3212-3222. https://doi.org/10.1016/j.ces.2011.02.029

[18] Gerlach, D., N. Alleborn, V. Buwa, and F. Durst. "Numerical simulation of periodic bubble formation at a submerged orifice with constant gas flow rate." *Chemical Engineering Science* 62, no. 7 (2007): 2109-2125. https://doi.org/10.1016/j.ces.2006.12.061

[19] Yan, Kai, and Defu Che. "A coupled model for simulation of the gas-liquid two-phase flow with complex flow patterns." *International Journal of Multiphase Flow* 36, no. 4 (2010): 333-348. https://doi.org/10.1016/j.ijmultiphaseflow.2009.11.007

[20] Li, Yong, Jianping Zhang, and Liang-Shih Fan. "Discrete-phase simulation of single bubble rise behavior at elevated pressures in a bubble column." *Chemical Engineering Science* 55, no. 20 (2000): 4597-4609. https://doi.org/10.1016/S0009-2509(00)00089-0
[21] Della Rocca, G., and Guillaume Blanquart. "Level set reinitialization at a contact line." *Journal of Computational Physics* 265 (2014): 34-49. https://doi.org/10.1016/j.jcp.2014.01.040
[22] Fan, Wenyuan, Yawei Sun, and Hui Chen. "Bubble Volume and Aspect Ratio Generated in Non-Newtonian Fluids." *Chemical Engineering & Technology* 37, no. 9 (2014): 1566-1574. https://doi.org/10.1002/ceat.201400083
[23] Agarwal, Shashwat S., Kunal Kumar, Laltu Chandra, and Pradyumna Ghosh. "Improved wake velocity distribution behind a rising bubble for isothermal and thermally stratified liquid layers." *Journal of Heat Transfer* 144, no. 7 (2022): 073701. https://doi.org/10.1115/1.4054413
[24] Rashid, Farhan L., Emadq Hussein, Ahmed Kadhim Hussein, and Obai Younis. "Parametric study of single air bubble rising through different salinity water column using volume of fluid (VOF) technique." *Journal of Engineering Science and Technology* 18, no. 1 (2023): 671-684.
[25] Webber, Norman Bruton. *Fluid Mechanics for Civil Engineers*. Routledge, 2018. https://doi.org/10.1201/9781315273426
[26] COMSOL. *COMSOL Multiphysics Reference Manual, version 5.3*. COMSOL AB: Stockholm, Sweden, 2017.
[27] Khalaf, Abbas Fadhil, Farhan Lafta Rashid, Hayder I. Mohammed, Ali Basem, Hussein Rasool Abid, and Mudhar A. Al-Obaidi. "Numerical Unveiling the Dynamics of Glycerin-Water Mixing: Insights into Compatibility and Behavior." *Journal of Advanced Research in Numerical Heat Transfer* 16, no. 1 (2024): 35-56. https://doi.org/10.37934/arnht.16.1.3556
[28] Jweeg, Mohsen, Emad Qasem Hussein, Farhan Lafta Rashid, and Ali Basem. "Investigation of Two-Way Fluid-Structure Interaction of Blood Flow at Different Temperature using CFD." *Journal of Advanced Research in Applied Sciences and Engineering Technology* 36, no. 2 (2023): 120-130. https://doi.org/10.37934/araset.36.2.120130
[29] Kadhum, Zahraa Mohammed, Mohammed Wahhab Aljibory, and Farhan Lafta Rashid. "Numerical simulation for the effect of air bubble injection in wavy pipe solar collector." In *AIP Conference Proceedings*, vol. 2977, no. 1. AIP Publishing, 2023. https://doi.org/10.1063/5.0182540
[30] Rashid, Farhan Lafta, Ali Basem, Abbas Fadhil Khalaf, Mudhar A. Al-Obaidi, Ahmed Kadhim Hussein, Bagh Ali, and Obai Younis. "Air Bubble Position Effect on Phase Change Material Melting in a Semi-Cylindrical Container: A Thermal Analysis." *Mathematical Modelling of Engineering Problems* 10, no. 6 (2023): 2281-2290. https://doi.org/10.18280/mmep.100644
[31] Al-Gaheeshi, Asseel M. Rasheed, Farhan Lafta Rashid, and Hayder I. Mohammed. "Dynamics of single bubble ascension in stagnant liquid: An investigation into multiphase flow effects on hydrodynamic characteristics using computational simulation." *Physics of Fluids* 35, no. 12 (2023). https://doi.org/10.1063/5.0174622
[32] Rashid, Farhan Lafta, Ali Basem, Mudhar A. Al-Obaidi, Sarah Abbas Jawad, Ahmed Kadhim Hussein, Bagh Ali, and Mohamed Bechir Ben Hamida. "An Examination of Air-Bubble Injection Mechanisms for Optimising Heat Transfer in Industrial Applications." *International Journal of Heat & Technology* 41, no. 5 (2023). https://doi.org/10.18280/ijht.410513
[33] Jawad, Sarah Abbas, Zeina Ali Abdul Redha, and Farhan Lafta Rashid. "Thermal performance of flat plate solar water collector using air bubble injection." In *AIP Conference Proceedings*, vol. 2651, no. 1. AIP Publishing, 2023. https://doi.org/10.1063/5.0133663
[34] Khalaf, Abbas Fadhil, Farhan Lafta Rashid, Ali Basem, and Mohammed H. Abbas. "Numerical Study of the Effect of Air Bubble Location on the PCM Melting Process in a Rectangular Cavity." *Mathematical Modelling of Engineering Problems* 10, no. 1 (2023). https://doi.org/10.18280/mmep.100109
[35] Rashid, Farhan Lafta, Shaheed Mahdi Talib, and Ahmed Kadhim Hussein. "An Experimental Investigation of Double Pipe Heat Exchanger Performance and Exergy Analysis Using Air Bubble Injection Technique." *Jordan Journal of Mechanical & Industrial Engineering* 16, no. 2 (2022).
[36] Talib, Shaheed Mahdi, Farhan Lafta Rashid, and Muhammad Asmail Eleiwi. "The effect of air injection in a shell and tube heat exchanger." *Journal of Mechanical Engineering Research and Developments* 44 (2021): 305-317.
[37] Altaie, Arkan, Moayed R. Hasan, and Farhan Lafta Rashid. "Numerical investigation in a circular tube to enhance turbulent heat transfer using opened rings-triangular cross section." *Journal of Babylon University/Engineering Sciences* 23, no. 3 (2015): 798-807.
[38] Altaie, Arkan, Moayed R. Hasan, and Farhan Lafta Rashid. "Numerical heat transfer and turbulent flow in a circular tube fitted with opened rings having square cross section." *Journal of Basic and Applied Scientific Research* 4, no. 11 (2014): 28-36.
[39] Mammadov, Ibrahim, Geylani Panahov, Sayavur Bakhtiyarov, and Parviz Museibli. "Investigation of the Effect of Mutual Diffusion on Hydrodynamic Parameters under Fluid Displacement." *Journal of Advanced Research in Fluid Mechanics and Thermal Sciences* 118, no. 1 (2024): 39-51. https://doi.org/10.37934/arfmts.118.1.3951

[40] Sarma, Gobburu Sreedhar, Gobburu Venkata Subbaiah, Ganji Narender, Dhonthi Srinivas Reddy, Dontula Shankaraiah, and Marla Umakanth. "Exploring Unsteady Three-Dimensional Casson Fluid Flow through a Stretching Surface with Heat Source/Sink: A Numerical Investigation." *Journal of Advanced Research in Fluid Mechanics and Thermal Sciences* 118, no. 1 (2024): 116-131. https://doi.org/10.37934/arfmts.118.1.116131

[41] Turton, R., and O. Levenspiel. "A short note on the drag correlation for spheres." *Powder Technology* 47, no. 1 (1986): 83-86. https://doi.org/10.1016/0032-5910(86)80012-2

[42] Mei, Renwei, and J. F. Klausner. "Shear lift force on spherical bubbles." *International Journal of Heat and Fluid Flow* 15, no. 1 (1994): 62-65. https://doi.org/10.1016/0142-727X(94)90031-0